JOURNAL OF
PALEONTOLOGY
A PUBLICATION OF THE

Paleontological
SOCIETY

A new marrellomorph arthropod from southern Ontario: a rare case of soft-tissue preservation on a Late Ordovician open marine shelf

Joseph Moysiuk,[1,2]* Alejandro Izquierdo-López,[1,2] George E. Kampouris,[3] and Jean-Bernard Caron[1,2,4]

[1]Department of Ecology and Evolutionary Biology, University of Toronto, 25 Willcocks Street, Toronto, Ontario M5S 3B2, Canada <joe.moysiuk@mail.utoronto.ca> <ai.lopez@mail.utoronto.ca> <jcaron@rom.on.ca>
[2]Department of Natural History, Royal Ontario Museum, 100 Queen's Park, Toronto, Ontario M5S 2C6, Canada
[3]St Isidore, Ontario, K0C 2B0, Canada <georgekamp@bell.net>
[4]Department of Earth Sciences, University of Toronto, 22 Russell Street, Toronto, Ontario, M5S 3B1, Canada

Abstract.—Ordovician open marine Lagerstätten are relatively rare and widely dispersed, producing a patchy picture of the diversity and biogeography of nonmineralized marine organisms and challenging our understanding of the fate of Cambrian groups. Here, for the first time, we report soft-bodied fossils, including a well-preserved marrellomorph arthropod, fragmentary carapaces, and macroalgae, from the Late Ordovician (Katian) Upper Member of the Kirkfield Formation near Brechin, Ontario. The unmineralized elements and associated exceptionally preserved shelly biota were entombed rapidly in storm deposits that smothered the shallow, carbonate-dominated shelf. The marrellomorph, *Tomlinsonus dimitrii* n. gen. n. sp., is remarkable for its ornate, curving cephalic spines and pair of hypertrophied appendages, suggesting a slow-moving, benthic lifestyle. Reevaluation of marrellomorph phylogeny using new data favors an arachnomorph affinity, although internal relationships are robust to differing outgroup selection. Clades Marrellida and Acercostraca are recovered, but the monophyly of Marrellomorpha is uncertain. The new taxon is recovered as sister to the Devonian *Mimetaster* and, as the second-youngest known marrellid, bridges an important gap in the evolution of this clade. More generally, the Brechin biota represents a rare window into Ordovician open marine shelf environments in Laurentia, representing an important point of comparison with contemporaneous Lagerstätten from other paleocontinents, with great potential for further discoveries.

UUID: http://zoobank.org/884589d0-08f7-4398-ab42-1f5d459be9e9

Introduction**

The Cambrian fauna has long been recognized as distinct from the later Paleozoic fauna (Conway Morris, 1989), notably thanks to soft-bodied elements recovered from Burgess Shale-type biotas in the former (Gaines et al., 2008; Gaines, 2014). However, more recent fossil discoveries from Konservat Lagerstätten around the world have demonstrated the persistence of select members of the Cambrian fauna into the mid to late Paleozoic. Important examples include diverse organisms from the early Ordovician (Tremadocian–Floian) Fezouata Lagerstätte (Van Roy et al., 2010), the Silurian (Pridolian) Herefordshire Lagerstätte (Siveter et al., 2020), and the early Devonian (Pragian to Emsian) Hunsrück Slate (Rust et al., 2016), among others. Nonetheless, the record of Burgess Shale-type faunas in post-Cambrian deposits remains sparse and patchy, not least because of the decrease in abundance

of Lagerstätten from open marine environments after the Cambrian (Orr, 2014; Muscente et al., 2017). This presents a major challenge for understanding the geographic distribution and ultimate decline of biotas of Cambrian origin through the Paleozoic.

One of the most distinctive classes belonging to the Cambrian fauna is Marrellomorpha, rare arthropods with unmineralized cuticle. Their distribution is restricted to Cambrian–Devonian Konservat Lagerstätten, but even here they occur only sporadically (Aris et al., 2017). Where they do occur, however, they range from among the most abundant species (Whittington, 1971; Caron and Jackson, 2008; Kühl and Rust, 2010) to an exceedingly rare element of the fauna (Liu, 2013). Two orders have been recognized within Marrellomorpha: Marrellida and Acercostraca (Rak et al., 2013). Members of the former are characterized by cephalic shields with two or three pairs of extremely elongate spinous projections and two to three pairs of uniramous cephalic appendages, while the latter possess large ovoid carapaces that cover the entire dorsal side of the animal and up to five pairs of cephalic appendages, the posteriormost one with a distinct filiform endopod. Both are united in possessing uniramous antennules and a multisegmented trunk

---

*Corresponding author
**This article has been updated since its original publication to correct mismatched figure captions. See https://doi.org/10.1017/jpa.2022.38.

CrossMark

bearing biramous appendages with exopods ornamented with medially directed setae (Rak et al., 2013). To date, four species of marrellids (Whittington, 1971; Kühl and Rust, 2010; Rak et al., 2013; Aris et al., 2017) and three acercostracans (Siveter et al., 2007; Kühl et al., 2008; Legg, 2016a) have been formally described, and at least one additional undescribed species of marrellid has been figured (Van Roy et al., 2010). In addition to these, the smaller and less well-known *Skania* and *Primicaris* have been suggested to have acercostracan affinities (Legg, 2015, 2016a) while other putative marrellids are represented by isolated fragments (Haug et al., 2012; Legg, 2016b). *Marrella splendens* Walcott, 1912 from the Cambrian remains the most abundant and well-known marrellomorph (Whittington, 1971; García-Bellido and Collins, 2006).

Despite the relative wealth of morphoanatomical information, the phylogenetic affinities of marrellomorphs have been problematic. In line with traditional views (Whittington, 1971; Kühl et al., 2008), some phylogenetic analyses in the past decade have found marrellomorphs to be arachnomorphs, allied closely with artiopodans (Aria and Caron, 2017b; Moysiuk and Caron, 2019) or, more unexpectedly, pycnogonids (Vannier et al., 2018). Alternatively, marrellomorphs have been considered either stem mandibulates (Legg et al., 2013; Legg, 2015) or stem "crustaceans" (Siveter et al., 2007; Ortega-Hernández et al., 2013) because of suggested homology of the carapace in acercostracans with that of certain early mandibulates and the presence of tergopleural rings and multisegmented exopods with medially directed lamellar setae, at least in marrellids (see also Haug et al., 2009). Finally, positions in the euarthropod stem group have also been suggested (Haug et al., 2012; Aria and Caron, 2017a). The monophyly of Marrellomorpha has been favored in the most recent literature although this has also been questioned (Siveter et al., 2007). These broad discrepancies pose a challenge for rooting the marrellomorph tree.

Here, for the first time, we describe the occurrence of soft-bodied fossils, including a specimen representing a new genus and species of marrellomorph arthropod, from shallow marine deposits of the Late Ordovician (early Katian) Kirkfield Formation (Paton and Brett, 2020) of southeastern Ontario. Referred to as the Brechin Lagerstätte, this locality has already been made famous by its exceptionally preserved echinoderm-dominated assemblages of biomineralizing organisms (Brett and Liddell, 1978; Cole et al., 2018, 2020). This finding represents a rare example of soft-tissue preservation in an Ordovician open shelf environment in association with a typical "shelly" marine biota. The marrellomorph is particularly significant as the first post-Cambrian representative found in Laurentia, and we take this finding as an opportunity to reevaluate marrellomorph systematics.

Geological setting

The marrellomorph specimen and other soft-bodied elements, including algae and potential arthropod carapaces, were collected from a study site exposing units of the Upper Member of the Kirkfield Formation in Tomlinson Quarry near Brechin, Ontario, Canada. This formation makes up the middle portion of the Simcoe Group, which records the widespread development of the Trenton Carbonate Platform in the epeiric seas along the southeastern margin of Laurentia (Brookfield and Brett, 1988; Paton and Brett, 2020). The Sandbian–Katian boundary is identified in the Lower

Member of the Kirkfield Formation, with the remainder of the formation being deposited in the earliest Katian (Paton and Brett, 2020). The Kirkfield Formation is dominated by carbonate facies, representing offshore shoal to shallow marine environments (around tens of meters of water); however, thin intercalations of K-bentonites and storm-deposited silty shales record occasional input of volcanic ash and other terrigenous material from the nearby Taconic Mountains (Brookfield and Brett, 1988).

The study area (approximately 44°35.496′N, 79°5.626′W) consists of biohermal communities established on hardground surfaces within a complex of sedimentary structures that follows a paleocurrent-aligned submarine ridge situated along a northeast to southwest line of strike, visible in outcrop. The ridge formed a subtle positive topographic feature at the northern margin of the biohermal zone and exerted strong controls over the formation and subsequent development of a range of structures, notably the complex hardground surfaces that formed the substrate for the diverse echinoderm–bryozoan-dominated fauna (Paton et al., 2019). The basal hardground (Unit a) and tiered hardground mounds (Units b and c) were repeatedly buried by up to 11 discrete obrution beds that are nonuniformly present across the study area, depending on local variations in depth and distance from the marginal ridge where all beds thin, pinch out, and grade into each other (Fig. 1.1–1.3). The local stratigraphy has been examined comprehensively (Paton et al., 2019; Paton and Brett, 2020), and the diverse echinoderm faunas have been the focus of several recent publications (e.g., Cole et al., 2018, 2019, 2020; Wright et al., 2020).

Of primary interest here are two shale horizons, Beds 1 and 3 (Fig. 1.1, 1.2), which preserve remains of nonmineralized fauna and flora. Bed 1 is soft brown-grey organic-rich shale, present only in the deepest mound basins, that covered robust echinoderm–bryozoan bioherms at their peak development and diversity. Preservation of nonmineralized elements is common, but they are fragmentary. Deposition of Bed 2, cross-bedded siltstone up to 15 cm thick, subsequently buried much of the hardground surface except for protruding mounds from units b and c, around which firmground communities locally reestablished. No soft-bodied elements are found in this bed. Bed 3, from which the marrellomorph was retrieved, consists of up to 10 cm of soft-grey shale grading to a hard brown-grey silty shale due to coarser material accumulating closer to the marginal ridge. This represents a major burial event that wiped out the recovering bioherms, resulting in crinoids being uprooted, decapitated, and buried with their stems oriented to the south. Large (100–300 μm) clusters of pyrite crystals are common. Soft-tissue preservation has been encountered thus far only in Tomlinson Quarry, but Bed 3 is laterally extensive at least to Carden Quarry (see Paton and Brett, 2020). Other shale layers are present (Beds 5, 7, 9), but none has thus far yielded soft-bodied fossils.

Cooccurring with the marrellomorph in Bed 3 are macroalgae, carapaces, and other indeterminate remains of nonbiomineralizing organisms, suggesting that conditions were conducive to soft-tissue preservation (Fig. 2). Bed 3 also hosts a diverse shelly marine fauna, including various trilobites, echinoderms, bryozoans, mollusks, conulariids, and receptaculitids, as well as trace fossils (Fig. 1.4; Supplementary Text, Supplementary Table 1). Fossils are abundant only around mound-adjacent basins where Bed 3 reaches its thickest.
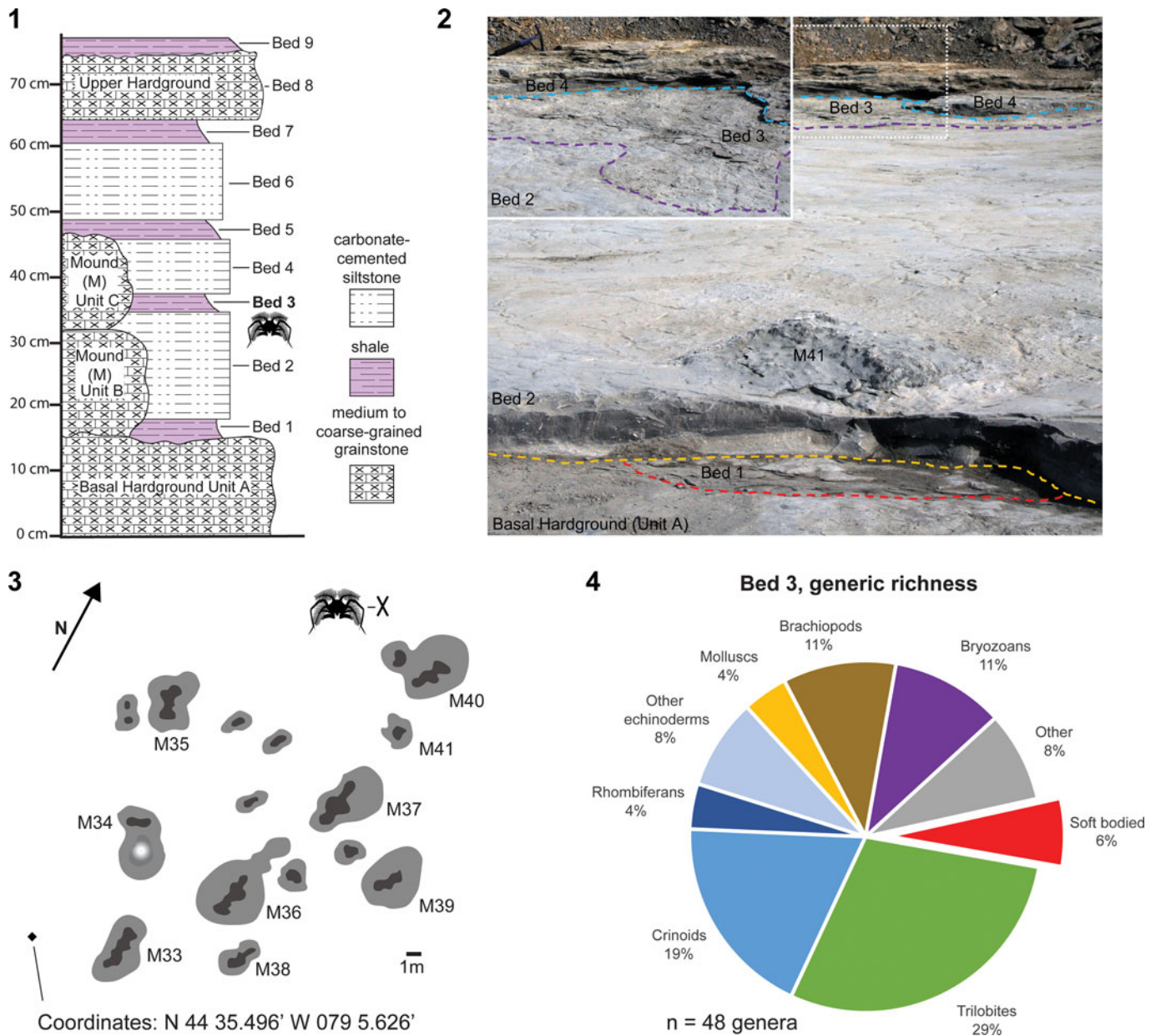
Figure 1. Brechin Lagerstätte locality information. (**1**) Stratigraphic column in the study area, modified after Paton et al. (2019). (**2**) Photographs of the site, looking east, showing the beds in which soft-tissue preservation has been observed and their relationship to the basal hardground and mound/basin structures, with hammer for scale. (**3**) Topographic map of the main study plot, with the location of ROMIP 66233 marked with an X; high relief mounds (prefix M) are numbered and shaded dark while surrounding basins are shaded lighter. (**4**) Generic richness subdivided by major fossil group in Bed 3 from the study plot; see supplementary text for details.

Materials and methods

In the following, we detail methods involved in field data collection, elemental mapping, and phylogenetic analyses.

Field collection.—A collected surface area of ~85 by 30 meters on a platform near the top of Tomlinson Quarry was available for excavation and study (Fig. 1.3). At least 20% of the soft and friable Bed 3 shale was lost due to wastage during excavation. The fossil abundance data reported in this paper reflects collections made from the remaining portions of Bed 3 in the study site, with greatest collecting intensity in the thickest mound-adjacent fossil-rich areas. Following the unexpected discovery of the marrellomorph in a fossil-poor section of shale between mounds, ~700 m^2 of surrounding shale was excavated more systematically. Taxon abundances are reported in Supplementary Table 1 but must be interpreted cautiously considering the uneven sampling approach.

Elemental mapping.—The composition of the marrellomorph was investigated with elemental mapping, performed with an environmental scanning electron microscope (FEI Quanta 200 FEG) equipped with an energy scanning spectroscopy (EDS) X-ray detector and octane plus silicon drift detector at the University of Windsor Great Lakes Institute for Environmental Research, Canada. Imaging analyses were

Figure 2. Representative biota from Brechin Lagerstätte. (**1**) ROMIP 66259, branching macroalga associated with the crinoid *Reteocrinus*, recovered from Bed 3. (**2**) ROMIP 66258, partial arthropod carapace, recovered from Bed 3. (**3**) ROMIP 65095, large slab covered in mineralized fauna, recovered from Bed 1 near Mound 37. (**1, 2**) Scale bars = 10 mm; (**3**) scale bar = 50 mm.

conducted with the following operating conditions: fixed average working distance of 10.3 mm (minor variation across specimen due to differences in topography) for basic imaging and EDS, 12 kV beam accelerating voltage, 252 µA beam current at source, 70 Pa chamber pressure (low vacuum), 30 µm aperture for imaging, and 40 µm aperture for EDS.

Phylogenetic methods.—The objective of our phylogenetic analysis was to build upon previous work on marrellomorphs (Rak et al., 2013; Legg, 2015, 2016a; Aris et al., 2017) but also to critically review all relevant characters, compare additional phylogenetic methods, and test the influence of competing outgroup hypotheses. Rather than using a major panarthropod phylogeny, (e.g., Legg, 2016a), we favored a marrellomorph-centric data set that would allow us to test the sensitivity of patterns of character evolution and ingroup relationships under different outgroup hypotheses. We therefore chose Aris et al. (2017) as our primary dataset of reference.

Our new phylogenetic matrix consists of 19 taxa and 44 characters and includes substantial corrections and modifications and new outgroups based on recent advances. More specifically, we removed noninformative and redundant characters as well as any whose definitions we considered to be insufficiently specific or poorly justified (see Supplementary Text). Since the position of Marrellomorpha among arthropods has been controversial, we employed multiple outgroups and used topological constraints to investigate how differing outgroup relationships might affect the ingroup. We selected *Kylinxia* (stem Euarthropoda; Zeng et al., 2020), *Waptia* (total group Mandibulata; Vannier et al., 2018), *Tokummia* (total group Mandibulata; Aria and Caron, 2017a), *Mollisonia* (stem Euchelicerata; Aria and Caron, 2019), *Eoredlichia* (Artiopoda; Hou et al., 2008), *Haliestes* (Pycnogonida; Siveter et al., 2004), and *Palaeoisopus* (Pycnogonida; Bergström et al., 1980) as well-known representatives of major outgroups. The trees were rooted on *Kylinxia*. We also included the problematic taxon *Aquilonifer* (Briggs et al., 2016) as in one previous study this was found to be possibly allied to marrellomorphs (Vannier et al., 2018). We specifically excluded some larval crustaceomorph taxa previously used as outgroups due to the known problems of incorporating different developmental stages in the same phylogeny (Sharma et al., 2017).

Our main analyses made use of the inapplicable state-corrected Parsimony approach (Brazeau et al., 2019) available in the R 4.1.0 (R Core Team, 2020) package TreeSearch 0.4.3.9010 (Smith, 2018), which relies on MorphyLib (Brazeau et al., 2017). Additional functions were supplied from packages ape 5.5 (Paradis et al., 2004), phangorn 2.7.0 (Schliep, 2011), TreeTools 1.4.5 (Smith, 2019a), strap 1.4 (Bell and Lloyd, 2015), and extraDistr 1.9.1 (Wolodzko, 2020). R code is available in supplementary files. For each analysis, we used 100 independent searches starting from random trees, with 3×6 initial TBR iterations followed by 12 rounds of Parsimony ratchet with six TBR iterations each, and finishing with 3×6 more TBR iterations. The maximum number of hits was set to 100. Analyses were performed under equal and implied weights, sampling concavity constants for the latter from a discrete gamma distribution with shape and size parameters equal to 3 with an additive constant of 2, chosen to sample the range of recommended values (Smith, 2019b). In addition to these

unconstrained analyses, we ran two equal-weights analyses with topological constraints to enforce the monophyly of Chelicerata exclusive of marrellomorphs and a sister group relationship between mandibulates and marrellomorphs. Jackknife resampling was performed 1,000 times to estimate clade support, using 2×6 starting iterations of TBR followed by five ratchet iterations, with six TBR iterations each, finishing with 3×6 TBR iterations per round. The maximum number of hits was set to 20.

We also performed standard Fitch Parsimony analysis in TNT 1.5 (Goloboff and Catalano, 2016) using 1,000 searches from random starting trees. We used five ratchet iterations and five rounds of tree fusing up to 50 hits of the best tree length, otherwise maintaining default xmult search settings. Results under implied weights (concavity = 3 and 10) resulted in identical consensus trees, so only the equal-weights result is shown. Jackknifing was performed 1,000 times using xmult settings with 100 replicates each and five ratchet iterations.

Finally, we performed Bayesian analysis in MrBayes 3.2.6 (Ronquist et al., 2012) using an Mkv + gamma model (Lewis, 2001). Four chains starting from random trees were run for 3×10^{6} generations, sampling every 1,000 generations, with a burn-in fraction of 20%. Convergence was verified in Tracer 1.7.1 (Rambaut et al., 2014). We also performed two analyses with the same topological constraints detailed in the preceding.

To investigate character optimization over the resulting trees, we used Parsimony ancestral state reconstruction in Mesquite 3.40 (Maddison and Maddison, 2018).

Repository and institutional abbreviation.—All specimens figured in this study are reposited in the Royal Ontario Museum Invertebrate Palaeontology (ROMIP) collections.

Systematic paleontology

Phylum Euarthropoda Lankester, 1904
Class Marrellomorpha Beurlen, 1930
Order Marrellida [nom. correct. Størmer, 1959, pro Marrellina Raymond, 1920]

Diagnosis.—Euarthropod with cephalic shield extending into at least two pairs of extremely elongated lateral spines. Some cephalic spines bearing secondary spines. First and second cephalic appendages uniramous. Trunk subequal to or shorter than cephalic spines, composed of more than 25 segments. Each trunk segment consisting of a short tergopleural ring and a pair of biramous appendages, with endopods bearing blunt subtriangular endites and highly subdivided exopods (~15 or more podomeres), each emitting elongated lamellae. Terminal segment a small undifferentiated plate with no distinct telson or caudal rami.

Remarks.—Emended from Raymond (1920). Størmer (1959) later corrected the name but did not revise the diagnosis. Raymond's order included only the genus *Marrella* and the short original diagnosis was: "Form trilobite-like, pleural lobes reduced, endobases absent from coxopodites of body, pygidium a small plate." We here revise the diagnosis considering more recent discoveries and our phylogenetic character optimizations.

Family Mimetasteridae Birenheide, 1971

Type genus.—*Mimetaster* Gürich, 1931.

Other genera.—*Tomlinsonus* new genus.

Undescribed Moroccan marrellid.—Specimens of this taxon have been referred to as *Furca mauritanica* (nomen nudum), as informally described by Van Roy (2006), although they have been figured in several publications (e.g., Van Roy et al., 2015). Specimens in the ROMIP collection show the diagnostic traits of Mimetasteridae (see Phylogenetic results). Differences between the shield shape of the Moroccan taxon and *Furca bohemica* Fritsch, 1908 are sufficient to justify considering the former a new genus, but a formal description is beyond the scope of this paper.

Other putatively included genera.—*Furca* Fritsch, 1908: *F. bohemica*, as most recently described by Rak et al. (2013), has a mimetasterid-like shield, with anterolateral spines and elongate secondary spines on the anterior and posterior edges of both the anterolateral and posterolateral spines. However, other body parts for *Furca* are currently unknown, and thus, we regard the assignment of *Furca* to Mimetasteridae as tentative, contra Rak et al. (2013).

   '*Mimetaster*' *florestaensis* Aris et al., 2017 was considered as a species of *Mimetaster* because of its phylogenetic position. As with *F. bohemica*, the shield of '*M.*' *florestaensis* shows diagnostic traits of Mimetasteridae, but the absence of the trunk and appendages prevents a confident assessment of its affinity. Furthermore, we suggest that '*M.*' *florestaensis* presents important differences from *M. hexagonalis* Gürich, 1931, including shape of the cephalic shield, shape and orientation of the cephalic spines, and shape of the secondary spines. The two also differ widely in age (Ordovician versus Devonian). '*M.*' *florestaensis* may be more appropriately assigned to *Furca* or a new genus, but this is also beyond the scope of this paper.

Diagnosis.—Marrellids with anterolateral spines protruding from the shield, each carrying a row of secondary spines on both anterior and posterior margins. Mediolateral and posterolateral spines also bearing marginal secondary spines. Secondary spines elongate, digitiform. Shield extends ventrally into a large, ellipsoidal hypostome. Cephalon includes three appendage-bearing segments. Second pair of appendages stenopodous, uniramous, greatly enlarged compared with other limbs, subdivided into around nine podomeres. Terminal podomere elongated, flattened, sometimes may be subdivided. Subterminal podomere bearing a spine. Third pair of appendages stenopodous, uniramous. Trunk with 30 or more appendage-bearing segments.

Remarks.—Emended from Birenheide (1971). Mimetasteridae was originally diagnosed as for the type genus, by monotypy. Following new discoveries and phylogenetic analyses, the family has been expanded to include other taxa (Rak et al., 2013; Aris et al., 2017) but has not been formally emended up to now. We here revise the diagnosis considering phylogenetic character optimizations.

Genus *Tomlinsonus* new genus

Type species.—*T. dimitrii* n. sp., by monotypy.

Diagnosis.—As for type species, by monotypy.

Etymology.—In reference to Tomlinson Quarry, where the holotype was discovered.

Remarks.—As for species.

Tomlinsonus dimitrii new species
Figures 3–6

Holotype.—ROMIP 66233, part and counterpart, a nearly complete head and partial trunk remains preserved in ventral view, representing the only known specimen.

Diagnosis.—Mimetasterid with subhexagonal central shield bordered by narrow, backward-curving spines. Broad rounded notch between anterolateral and mediolateral spines. Elongate, digitiform secondary spines present on anterolateral and mediolateral spines, on both anterior and posterior margins, oriented at a slight acute angle to primary spines. Second pair of appendages extremely elongate with subterminal podomere bearing a spine about 30% as long as the terminal podomere. Terminal podomere flattened, elongated, and undivided with a blunt tip.

Occurrence.—Kirkfield Formation, Upper Member (Katian; *Corynoides americanus* Graptolite Biozone; *Amorphognathus tvaerensis* Conodont Biozone); Bed 3 of Tomlinson Quarry, southeastern Ontario, Canada.

Description.—The holotype consists of a partially visible cephalic shield, a pair of hypertrophied cephalic appendages, one smaller cephalic appendage, and traces of at least four minute trunk appendages (Figs. 3–4). The shale split irregularly through the specimen, but preparation of both part and counterpart revealed details of the cephalic spines and appendages, respectively.

   The cephalic shield (Fig. 3) measures about 13.5 mm long to the attachment of the hypertrophied appendages and about 9.6 mm wide at the point of maximal constriction between the anterolateral and mediolateral spines. A slightly darker, posteriorly tapering, fusiform medial region, extending nearly from the anterior margin of the shield to slightly beyond the attachment site of the hypertrophied appendages, may represent the hypostome. The anterolateral spines project forward from the central shield at an angle of ~40° to the midline, but they curve along the proximal third of their length to project laterally, nearly orthogonal to the sagittal axis. They measure approximately 3.4 mm wide at the base, tapering gradually over their length of about 31.6 mm, measured anteriorly. Approximately 27 digitiform secondary spines are visible on the anterior margins of the anterolateral spines. Partly preserved spines on the posterior margin indicate that there may have been a similar number of spines present (Figs. 3.1, 4.1). The secondary spines appear to be longest proximally, ranging from about 7.6 mm, but poorer preservation distally prevents confident measurement.

Figure 3. Overview of *Tomlinsonus dimitrii*, holotype, ROMIP 66233. (**1**) Composite image of part and counterpart. (**2**) Part. (**3**) Counterpart. Scale bars = 10 mm. Photos taken with specimen submerged in alcohol and polarized lighting. a.s = anterolateral spine; c.aX = cephalic appendage X; en = endopod of trunk appendage; hs = head shield; hy = hypostome; m.s = mediolateral spine; pX = podomere number X; s.s = secondary spine; sp = spine on p8 of hypertrophied limb.

Posterior to the anterolateral spines, the shield widens to about 14.4 mm, producing an overall subtrapezoidal shape. From here, the mediolateral spines project approximately orthogonal to the midline (Figs. 3, 4.3). They measure about 3.6 mm wide at the base and at least 38.2 mm along the anterior margin. The mediolateral spines curve sharply for the first third of their length, achieving an angle of ~15° posterolateral to the midline and then projecting roughly straight. Secondary spines also ornament the mediolateral spine, with ~30 along the anterior face and at least ~16 distally on the posterior face. The margins of
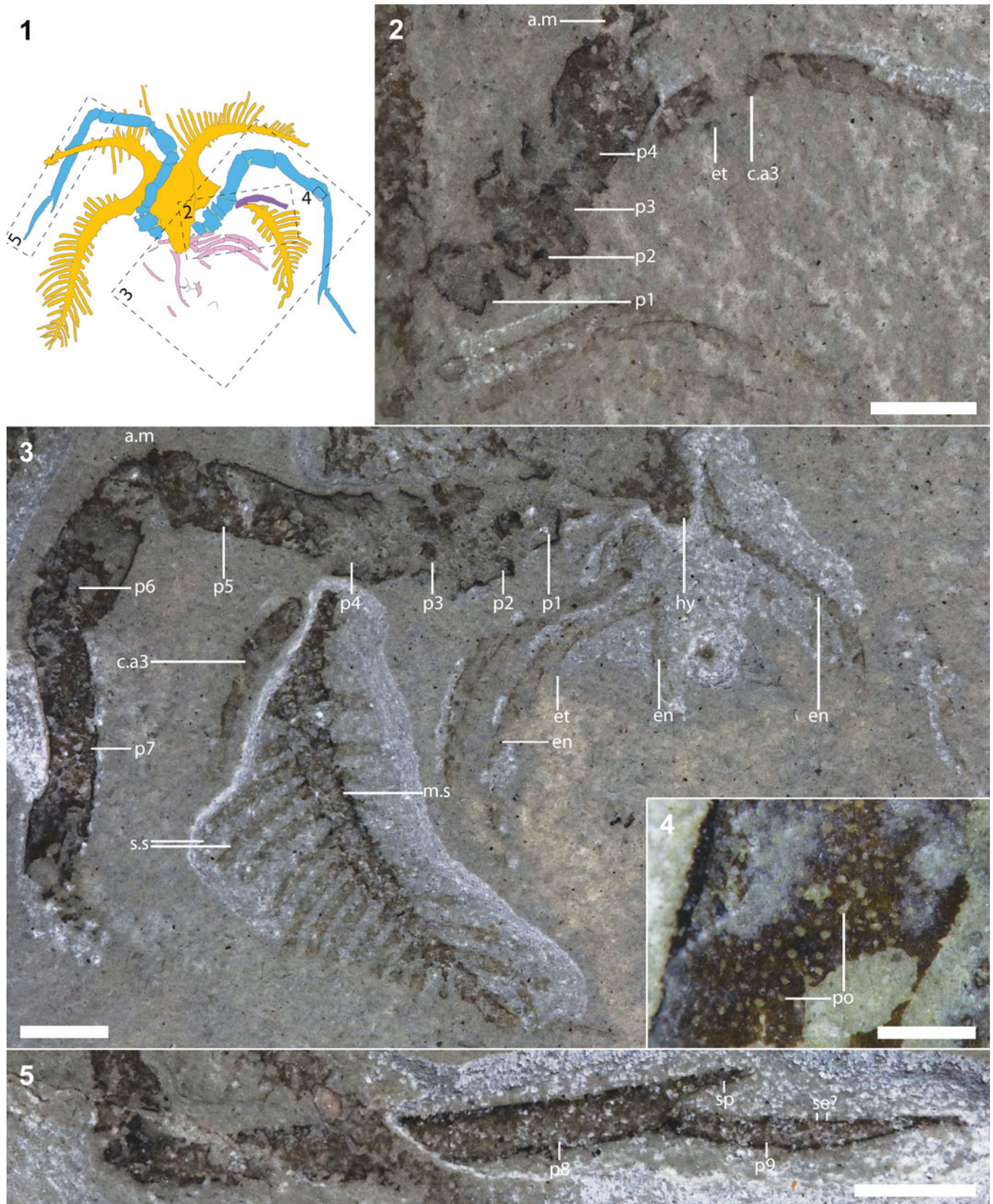
Figure 4. Closeup views of *Tomlinsonus dimitrii*, holotype, ROMIP 66233. (**1**) Line drawing of specimen (part–counterpart composite), with boxed areas representing numbered closeups in following panels. (**2**) Proximal part of hypertrophied appendage and other appendages on counterpart. (**3**) Appendages and mediolateral spine on part. (**4**) Closeup of well-preserved cuticle with pores on podomere 7. (**5**) Distal end of hypertrophied appendage on counterpart. (**2**, **3**, **5**) Scale bars = 4 mm; (**4**) scale bar = 1 mm. a.m = possible arthrodial membrane; et = endite; po = pores; se? = possible serrated margin; other abbreviations as in Figure 3.
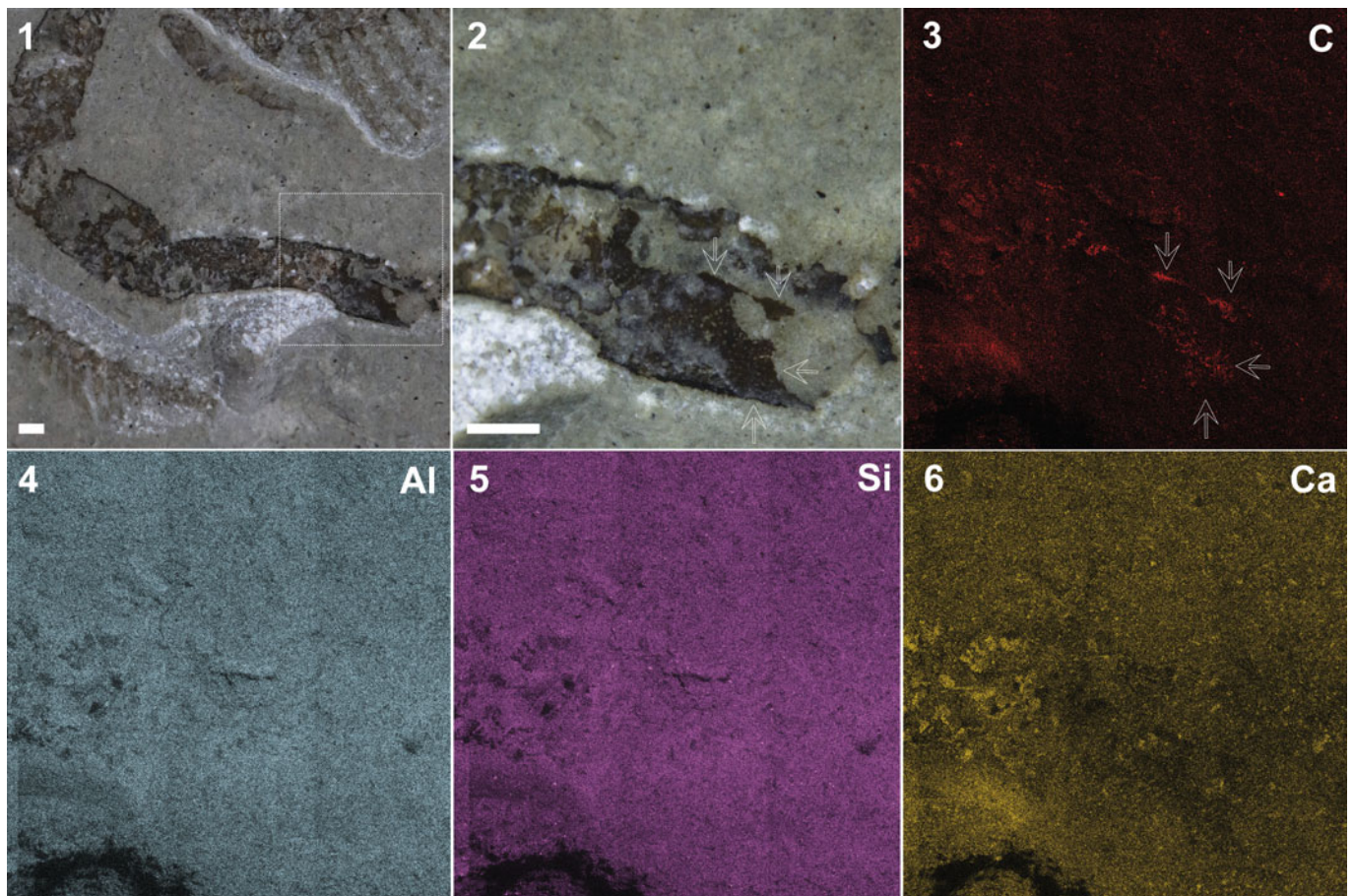
Figure 5. Elemental maps of the seventh podomere of a hypertrophied appendage of *Tomlinsonus dimitrii*. (**1**) Boxed region showing the location of the maps on the part. (**2**) Photograph of the mapped region with arrows indicating fragments of well-preserved cuticle; note the large crystals occupying central void on left side. (**3**) Carbon map with arrows pointing to cuticle fragments. (**4**) Aluminum map. (**5**) Silicon map. (**6**) Calcium map; note enrichment in crystals on the left. Scale bars = 1 mm.

the cephalic shield are not visible posterior to the mediolateral spines, so the presence of posterolateral spines, as found in other marrellids (Rak et al., 2013), cannot be confirmed.

The first pair of visible appendages are the hypertrophied pair (Figs. 3, 4). They consist of nine podomeres (P1–9) and are about 70.0 mm in total length, extending well beyond the cephalic spines even when partially bent. Small patches of cuticle are well preserved and show evidence of surface ornamentation consisting of small, rounded, closely spaced pores, ~50–70 µm in diameter (Fig. 4.4). The hypertrophied appendages attach behind and inward of the mediolateral spines. From here, one curves anteriorly and outward relative to the body, while the other bends inward over the head before turning outward. The attachment podomere (P1) is small (2.6 mm), ovoid, and bears no evidence of spines or a gnathobase. P2 is stout and subrectangular in profile, about 2.9 by 3.7 mm. P3 is extremely short and crescentic. P4 is rounded and tapers distally toward P5. P5 is elongate, and the distal end is inclined at about 25°, producing a strong bend in the appendage. P6 is longer and subrectangular in profile, about 7.5 by 3.4 mm. Small fields of carbon between P4, 5, and 6 may represent arthrodial membranes. P7 is about 11.2 by 2.2 mm. On the right appendage, it appears to be curved along its length, but this is likely an artefact of localized

deformation of the adjacent sediment. P8 is much longer and narrower than the preceding podomeres, at 16.5 by 1.3 mm, and is also preserved in a strongly bent orientation relative to P7. The distal inner margin of P8 projects into a straight spine, 2.9 mm long, parallel to the podomere long axis. P9 is an elongate, straight, flattened spine, possibly with marginal serrations, about 9.2 mm in length. P9 articulates in an outward direction, opposite to preceding podomeres. On the left appendage, the terminal podomere appears to twist along its length (Fig. 4.5), but this may be due to deformation.

Several incomplete appendages are also present (Fig. 4.2, 4.3). One moderately sized appendage on the right side, 1.0 mm wide, preserves four elongate subrectangular podomeres and protrudes from near the base of the hypertrophied appendage. Its proximal and distal ends are incomplete, but it seems likely it inserted just posterior to the hypertrophied appendage. One podomere bears a small, blunt, triangular endite, distally. At least three or four filamentous endopods, 0.5 mm wide, with traces of up to five elongate subrectangular podomeres are also visible on the right side. The proximalmost podomeres are relatively short and lacking any outgrowths. These are succeeded by at least four more elongate podomeres, each showing traces of a small, distal, spinose, blunt endite. We find no evidence of exopods. At least one more equivalent
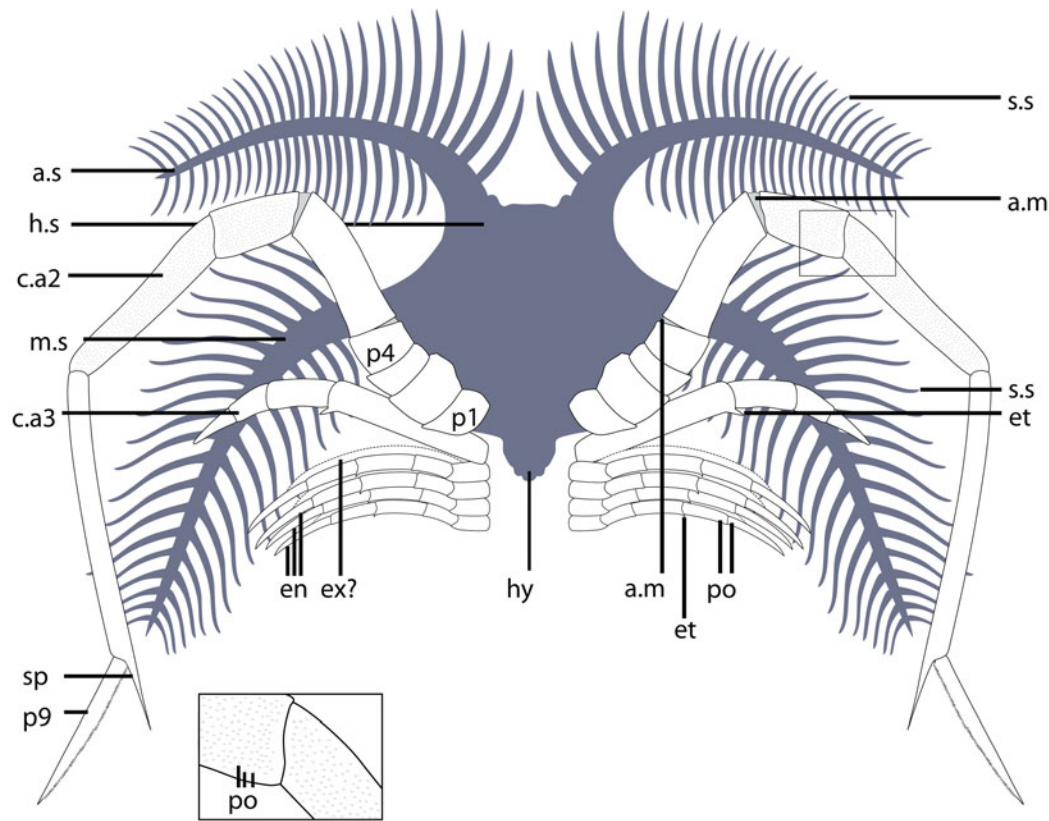
Figure 6. Reconstruction of *Tomlinsonus dimitrii*. (**1**) Line drawing showing major features. ex = trunk exopod; other abbreviations as in Figures 3 and 4. (**2**) Life reconstruction of *T. dimitrii*; art by Christian McCall.

appendage from the left side appears to be preserved folded over the midline while the base of another is visible posterior to the base of the hypertrophied appendage. These filamentous appendages clearly attach posterior to the two larger head appendages and are interpreted as belonging to the trunk region.

Etymology.—In recognition of Dimitri G. Kampouris, who emigrated from Egypt to Sudbury, Ontario, as a hard rock

miner and whose support and encouragement were necessary to carry out the study of the Brechin Lagerstätte.

Taphonomy.—The single marrellomorph specimen is dorsoventrally compressed but retains some dimensionality. Patchy brown layers of carbonaceous cuticle, sometimes retaining ornamentation, are preserved surrounding a central sediment-filled void (Fig. 5). This is reminiscent of the mode of preservation of, for example, eurypterid cuticles at other
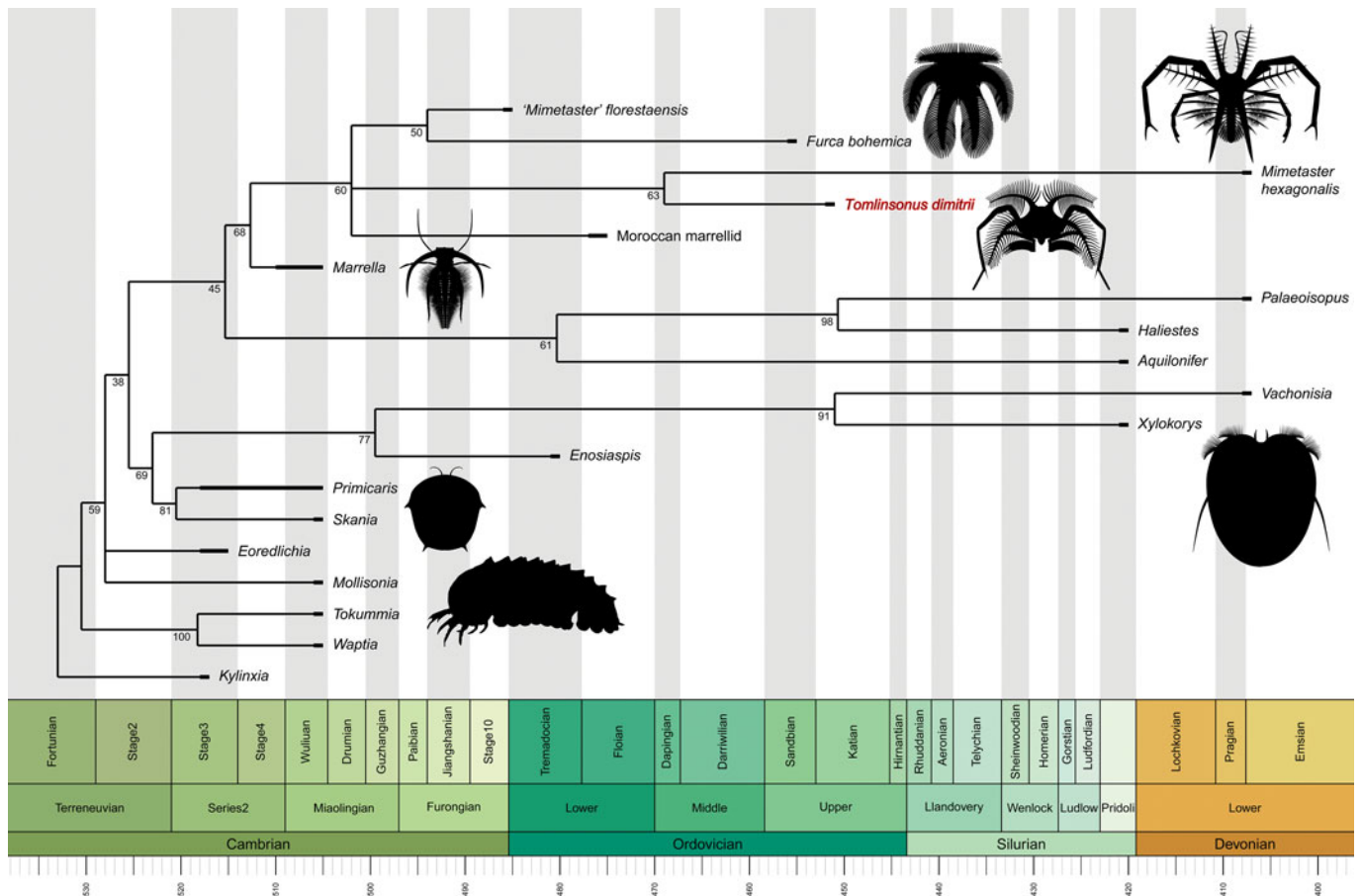
Figure 7. Phylogeny of marrellomorphs. Topology from equal weights analysis using inapplicable state-corrected parsimony. Node ages, intended for visual purposes, were generated in the R package strap using "equal" dating and a root length of 15, set to be roughly consistent with the earliest arthropod fossil record. See supplementary text for alternative topologies.

mid-Paleozoic Lagerstätten (Gupta and Briggs, 2011). In parts of the appendages, the central void also contains blocky crystals enriched in calcium and carbon (Fig. 5), presumably representing calcium carbonate, which must have precipitated within the enclosed environment formed by the cuticular remains before collapse. This is intriguingly similar to the otherwise unique mode of preservation of trilobite appendages exhibited at the Walcott Rust Lagerstätte (Brett et al., 1999); however, in the marrellomorph, this is evidently secondary to the carbonaceous mode of cuticle preservation. We observe no enrichment in magnesium, iron, or sulfur. Algae and carapaces cooccurring with the marrellomorph are preserved as brown to blackish traces and presumably exhibit an equivalent, primarily carbonaceous, mode of preservation.

Remarks.—*T. dimitrii* is the first marrellomorph to be formally described from the post-Cambrian of Laurentia and represents the second-youngest occurrence of Marrellida globally.

Phylogenetic results

We present the unconstrained inapplicable-corrected Parsimony result as our main tree (Fig. 7) with other trees available in Supplementary Text (Supplementary Figs. 1–3). Here we discuss the major similarities and differences between approaches.

In unconstrained Parsimony topologies, marrellomorphs are found within Arachnomorpha (Fig. 7; Supplementary Figs. 1, 2). Several potential synapomorphies allying marrellomorphs with other arachnomorphs are a head shield with a doublure and lateral spines, a ventral hypostome, well-developed endopods on all cephalic appendages, and the absence of caudal rami. The probable presence in *Xylokorys* of gnathobasic basipods (Siveter et al., 2007) also constitutes a connection as these have been argued to be an important arachnomorph synapomorphy (Aria and Caron, 2017b). A mandibulate affinity of marrellomorphs is not supported by any of our consensus topologies, except where constrained, although a marrellid–mandibulate relationship is represented in a minority of unconstrained Bayesian posterior trees (Supplementary Fig. 3; 0.30 probability). We note, however, that the unconstrained Maximum Clade Credibility tree (MCC) also recovers the presumably spurious result that pycnogonids are more closely related to mandibulates than to *Mollisonia*, presumably a result of limited outgroup taxon sampling. When the monophyly of Chelicerata is enforced, the MCC instead suggests weak support for Arachnomorpha. When a mandibulate + marrellomorph clade is constrained, the Bayesian approach produces a grouping of mandibulates and marrellids to the exclusion of acercostracans.

In addition, we find poor or ambiguous support for the monophyly of Marrellomorpha, with marrellids and

acercostracans frequently separated (as in Parsimony and unconstrained Bayesian MCC) or in a polytomy with other taxa (as in Bayesian majority rule consensus). Our unconstrained topologies surprisingly favor the paraphyly of Marrellomorpha with respect to pycnogonids, the latter most closely related to marrellids. These taxa are united, albeit with low support, by the loss of lateral compound eyes (excepting possibly in *Mimetaster*); differentiation of at least the second, and often third (excepting *Marrella*), cephalic appendages; the presence of cephalic endopods with more than seven podomeres (excepting *Marrella*); and possibly the loss of cephalic exopods. Previously proposed apomorphies of Marrellomorpha are the presence of a frontal rim on the head, which homologizes the general structure of the acercostracan carapace with the cephalic spines of the marrellids (Legg, 2016a), trunk multisegmentation, and a multipodomerous trunk exopod (Rak et al., 2013). It should be noted that the last of these is in fact unknown in acercostracans. Our parsimony topologies favor either convergence in the first two characters in acercostracans and marrellids or their loss in pycnogonids. The problematic *Aquilonifer* always resolves close to pycnogonids, regardless of constraints or treatment of inapplicability, but experimental removal of this taxon from the matrix does not impact other aspects of the topology (results not shown).

A clade of *Xylokorys*, *Vachonisia*, and *Enosiaspis*—Vachonisiidae sensu Legg (2016a)—is recovered in all trees, while a more inclusive acercostracan clade additionally containing *Skania* and *Primicaris* is typically recovered with lower support and is uncertain depending on outgroup constraints. While *Skania* and *Primicaris* appear commonly associated with acercostracans, the only reliable synapomorphies for this grouping are the relative enlargement of the trunk exopods and possibly the cephalic carapace.

Marrellida is well supported in all Parsimony analyses (Fig. 7; Supplementary Figs. 1,2) but receives relatively low posterior probability under a Bayesian approach. The presence of mediolateral and posterolateral spines bearing secondary spines are diagnostic for marrellids. Similarly, a clade of all marrellids excluding *Marrella*, Mimetasteridae sensu Rak et al. (2013), is recovered in all Parsimony analyses (supported by the presence of anterolateral spines) but not in the Bayesian majority rule consensuses (Supplementary Fig. 3). The Bayesian result appears to be due to alternative placements of *Furca bohemica* and '*Mimetaster*' *florestaensis* as basally diverging marrellids in some posterior trees (e.g., MCC trees). The missing appendicular data for these taxa are presumably responsible for this instability. *F. bohemica* and '*M.*' *florestaensis* are favored as sister taxa with weak support regardless of outgroup constraints. Presence of short anterolateral spines is the synapomorphy for these taxa. *Tomlinsonus dimitrii* n. gen. n. sp. is always found sister to *Mimetaster hexagonalis*, united by a similar subhexagonal cephalic shield and the conspicuous hypertrophied appendage.

Discussion

The discovery of *Tomlinsonus* has implications for understanding the evolution, mode of life, biogeography, and diversity of Marrellomorpha, among the most problematic of Paleozoic arthropods. Our findings also have more general significance

as a surprising case of soft-tissue preservation from an Ordovician open shelf environment.

Significance for marrellomorph ecology and evolution.— *Tomlinsonus* constitutes the second-youngest occurrence of a marrellid in the fossil record, helping to bridge the stratigraphic gap between earlier marrellids and the Devonian *Mimetaster*. Occurrence of a marrellomorph, a classic constituent of the Cambrian biota, in Ontario also demonstrates for the first time the persistence of this clade in Laurentia after the Cambrian. Along with reports from Ordovician deposits in Morocco (Van Roy et al., 2010), Wales (Legg, 2016b), Czech Republic (Rak et al., 2013), and Argentina (Aris et al., 2017) and from the Devonian of Germany (Kühl and Rust, 2010), this discovery demonstrates the broad post-Cambrian distribution of marrellomorphs and emphasizes their peak in generic diversity in the Ordovician.

The most remarkable aspect of the morphology of *Tomlinsonus* is the pair of hypertrophied appendages. These are virtually identical in form to the post-antennular appendages in *Mimetaster hexagonalis* (Fig. 8.3; Kühl and Rust, 2010) although they show the number and morphology of proximal and distal podomeres with greater clarity. A similar, though shorter, pair of appendages also appears to be present in the undescribed marrellid from the Fezouata Formation (Fig. 8.2). Mimetasterid second appendages differ in structure from the equivalent pair in *Marrella*, which are flattened, fringed laterally with rows of setae, and have been compared to the oar-like appendages of nektonic aquatic insects (Fig. 8.1; García-Bellido and Collins, 2006). While the pores visible on the cuticle of *Tomlinsonus* may represent setal attachment sites, their even distribution across the podomeres is suggestive of a sensory rather than locomotory function (Garm and Watling, 2013).

Despite the high number of podomeres, the postantennular appendage in mimetasterids is composed of mainly two elongated sections ending in a long distal podomere articulating outward. The proximal section, composed of short podomeres 1–5 probably served to lift the body and facilitate lateral movement, while the longer podomeres (P6–8) in the distal section elevated the body above the substrate. The arthrodial membrane between P5 and P6 may have allowed for a high range of rotation of the distal axis. This type of appendage is reminiscent of that of some pycnogonids, as previously noted (Kühl and Rust, 2010), and may have similarly functioned as pushing or pulling anchors enabling long strides and possibly direction changes, while the posterior appendages were used for forward propulsion (Schram and Hedgpeth, 1978). The pulling strategy in pycnogonids is dependent mostly on the presence of terminal claws. In at least *Tomlinsonus*, the terminal podomere appears to be a simple spine, but the additional spine on the subterminal podomere could have penetrated the substrate, providing traction. In this case, the outward-articulating, flattened terminal podomere may have been able to rest in plantigrade fashion on the substrate, distributing weight over a larger area. The situation may be convergent with the tarsal "feet" of many terrestrial arthropods (Kühl and Rust, 2010), although in *Tomlinsonus* this would more likely represent an adaptation to life on a soft marine substrate. Alternatively, the entire distal podomere could have been buried in the substrate, providing an anchor while the body shifts position, as takes place in the feeding process of
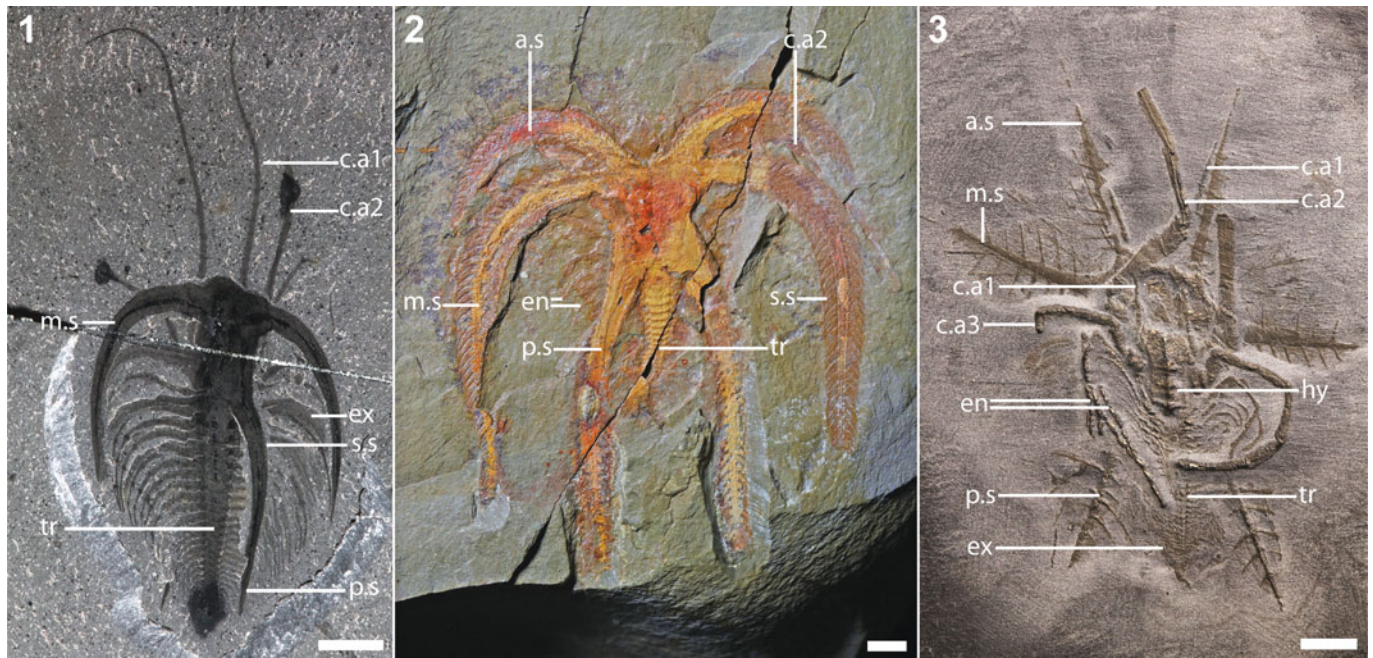
Figure 8. Comparative images of marrellids from other deposits. (**1**) ROMIP 61142, *Marrella splendens*, from the Burgess Shale. (**2**) ROMIP 63766, undescribed marrellid from the Fezouata Formation. (**3**) ROMIP 49452, *Mimetaster hexagonalis*, from the Hunsrück Slate. Scale bars = 4 mm. a.s = anterolateral spine; c.aX = cephalic appendage X; en = endopod of trunk appendage; ex = exopod; hy = hypostome; m.s = mediolateral spine; p.s = posterolateral spine; s.s = secondary spine; tr = trunk.

some pycnogonids (Manton, 1978). These similarities aside, the precise mode of locomotion in *Tomlinsonus* and other mimetasterids must have been somewhat different from that of other arthropods discussed given the presence of only a single pair of hypertrophied appendages.

Previous findings of marrellomorphs as stem group mandibulates relied on proposed homologies with Cambrian "crustaceomorph" larvae. Questions about the validity of these homology statements (Kühl et al., 2008; Haug et al., 2012) combined with the problems associated with coding different developmental stages in phylogenetic analyses render these results ambiguous. At least our Parsimony analyses with exclusively adult taxa favor an arachnomorph affinity. We caution that the small fraction of outgroup taxa and relevant characters sampled in our dataset are insufficient to provide robust support, as also reflected by our more ambiguous Bayesian results. More outgroup taxa will ultimately be needed to resolve marrellomorph affinities; however, we suspect that new fossil discoveries will also be essential given the high levels of conflicting phylogenetic signal that characterize this group.

The unexpected paraphyly of Marrellomorpha with respect to pycnogonids recovered in some of our analyses warrants discussion. Support for this relationship is relatively low, but the result is convergent with previous findings using a very different data matrix (Vannier et al., 2018). Despite obvious differences in gross morphology, some characteristics of marrellids, in particular, such as the loss of lateral compound eyes and the few-segmented head with uniramous agnathal appendages bearing more than seven podomeres, find commonality with pycnogonids. This hypothesis could have the radical implication that pycnogonid chelifores evolved convergently with euchelicerate chelicerae from a uniramous antennule. This is further suggested

by the recovery of *Aquilonifer* as the sister taxon to pycnogonids in several trees. Nonetheless, considering the bizarre morphologies of both pycnogonids and marrellomorphs, this result should be viewed cautiously. Given the relatively weak support for marrellomorph paraphyly, we retain Marrellomorpha for taxonomic purposes in this paper. We note that the internal relationships of marrellids and acercostracans remain stable when chelicerate monophyly (exclusive of marrellomorphs) is enforced.

Our analyses suggest revisions of the internal relationships of Marrellida. While '*Mimetaster*' *florestaensis* was previously found together in a polytomy with *M. hexagonalis* and the Fezouata marrellid, our analyses find some evidence for a closer affinity of the former with *Furca bohemica*. The original assignment to the genus *Mimetaster* was based entirely on the phylogenetic result, supported by a single vaguely defined character ("elongate anterior cephalic spines"). Provisionally, we suggest that reassignment to the genus *Furca* or to a new genus would be more in keeping with the evidence, acknowledging the present limitations imposed by incomplete preservation.

While *Tomlinsonus dimitrii* n. gen. n. sp. is phylogenetically closest to *M. hexagonalis*, it is morphologically and temporally distinct enough to warrant assignment to a new genus. It is also distinct from the Ordovician *Dyrnwynia conollyi* Legg, 2016b, which is known from a single putative mediolateral cephalic spine apparently lacking any secondary spines on the posterior margin (Legg, 2016b). *T. dimitrii*, by contrast, bears secondary spines on both margins of the mediolateral spine. Unfortunately, *D. conollyi* was too incomplete and problematic to be included in our phylogeny.

Soft-tissue preservation on a Late Ordovician open shelf.—The Brechin area is already famous for its exceptionally preserved

record of echinoderms, which in some beds were smothered rapidly in situ (Brett and Liddell, 1978; Cole et al., 2020). This paper constitutes the first report of soft-tissue preservation in the formation and the oldest such record in Ontario. While already meeting the broad criteria for consideration as a Konservat Lagerstätte (Seilacher et al., 1985), the preservation of soft tissues at Brechin cements this status in a more exclusive sense. More generally, this shows that the preservation of nonmineralized tissues is possible on the widespread Late Ordovician carbonate platforms of Laurentia.

Soft-bodied macrofossils remain rare at Brechin, with only six identifiable specimens recovered. While a considerable area of Bed 3 was examined, a systematic search for soft-bodied fossils was conducted only in a more limited area. Given also that nonmineralized fossils are difficult to discriminate against the matrix under outdoor lighting conditions, identification is challenging in the field. We think that more intensive sampling from intermound areas has great potential to reveal other soft-bodied organisms.

In contrast to the many marine shelf Lagerstätten of the Cambrian, most Laurentian Ordovician Lagerstätten such as Winneshiek (Briggs et al., 2018), William Lake and Airport Cove (Young et al., 2012), Big Hill (Lamsdell et al., 2016), and Kagawong (Stott et al., 2005), represent hostile, restricted, marginal marine settings with a low diversity of hardy taxa. Eurypterids, xiphosurans, phyllocarids, medusae, and unmineralized tubes tend to dominate these soft-bodied faunas. Far fewer Ordovician Lagerstätten have been reported from more distal marine shelf environments (Orr, 2014; Van Roy et al., 2015). Beecher's Trilobite Beds and related sites in New York are likely the most significant of those in Laurentia, exquisitely preserving the soft tissues of trilobites, ostracods, echinoderms, and several soft-bodied taxa yet to be described (Farrell et al., 2009). Here, the environment has been interpreted as generally dysoxic, with the fossil assemblage representing a specialized biota adapted to these conditions (Farrell et al., 2011). Cat Head, Manitoba, represents a similar case, preserving a diversity of sponges, macroalgae, and possible hydrozoans alongside typical Ordovician shelly biotas, but showing signs that the basin in which it resided may have been circulation restricted (Young et al., 2012). Another well-known marine shelf Lagerstätte, the Walcott Rust Quarry in New York, shows soft-tissue preservation largely confined to trilobite appendages (Brett et al., 1999). Finally, a few other examples of soft-tissue preservation in deep basinal environments demonstrate potential for further discoveries, but presently sampling has yielded only a low diversity of problematica (Macgabhann and Murray, 2010; Meyer et al., 2018; Peel et al., 2019). Thus, while all these sites provide critical insights, their biotas are not easily comparable to those of Cambrian Lagerstätten from open marine shelf environments.

Outside of Laurentia, the Fezouata biota of Morocco provides the best view of an Ordovician open shelf biota. Here, shelly and soft-bodied organisms characteristic of both Cambrian (e.g., radiodonts, lobopodians, marrellomorphs, nektaspids, paleoscolecids) and Paleozoic (e.g., horseshoe crabs, eurypterids, phyllocarids, various echinoderms, mollusks, and bryozoans) faunas occur together (Van Roy et al., 2015). A few other sparser assemblages may provide comparable

windows in other regions (e.g., Muir et al., 2014; Balinski and Sun, 2015; Botting et al., 2015; Hearing et al., 2016; Aris et al., 2017; Kimmig et al., 2019). The occurrence of *Tomlinsonus* in shallow marine deposits in Ontario, preserved alongside diverse echinoderms, trilobites, brachiopods, and bryozoans, provides a tentative connection with these other sites and indicates that marrellomorphs were likely typical members of Ordovician marine shelf communities. Being Katian in age, and thus younger than the aforementioned assemblages, this occurrence also lends further support to the notion that this type of fauna may have persisted broadly until at least the end-Ordovician extinction.

The Brechin Lagerstätte thus represents one of very few examples of soft-tissue preservation from an Ordovician open marine shelf and an important window into this environmental setting in Laurentia. While few examples of soft-tissue preservation have been collected to date, the lateral extent and repetitive nature of obrution events in the upper Kirkfield Formation offers a tantalizing hint that further exploration may yield more insights into the origin, biogeography, and longevity of distinctive soft-bodied fauna. This will provide an important complement to Silurian Lagerstätten of Ontario, which have already yielded rare elements of the Cambrian fauna, such as naraoiids and lobopodians, alongside more typical Paleozoic taxa (Caron et al., 2004; von Bitter et al., 2007). More broadly, our findings illustrate the potential for discovering cryptic cases of soft-tissue preservation among well-studied "shelly" biotas of the mid-Paleozoic.

Author contributions

Funding

Acknowledgments

and S. Berquist in particular for their interest and support. We thank M. Akrami for assistance in the ROMIP collections, S. Lackie for elemental maps, C. McCall for artistic reconstruction, M. Smith for assistance with the R package *TreeSearch* and for enabling constraint functionality, D. de Carle for discussions on phylogenetic approaches, C. Aria for comments on nomenclature, D. Rudkin for information on Lagerstätten of Ontario, and R. Lerosey-Aubril for helpfully providing a reference. We also appreciated constructive remarks from S. Zamora, J. Kimmig, and an anonymous reviewer. TNT is freely available thanks to the Willi Hennig Society.

Data Availability Statement

Data available from the Dryad Digital Repository: https://doi.org/10.5061/dryad.dfn2z353m

Supplementary materials are available from Zenodo: https://doi.org/10.5281/zenodo.5851832

References

Aria, C., and Caron, J.-B., 2017a, Burgess Shale fossils illustrate the origin of the mandibulate body plan: Nature, v. 545, p. 89–92.

Aria, C., and Caron, J.-B., 2017b, Mandibulate convergence in an armoured Cambrian stem chelicerate: BMC Evolutionary Biology, v. 17, p. 261.

Aria, C., and Caron, J.-B., 2019, A middle Cambrian arthropod with chelicerae and proto-book gills: Nature, v. 573, p. 586–589.

Aris, M.J., Corronca, J.A., Quinteros, S., and Pardo, P.L., 2017, A new marrellomorph euarthropod from the Early Ordovician of Argentina: Acta Palaeontologica Polonica, v. 62, p. 1–8.

Balinski, A., and Sun, Y., 2015, Fenxiang biota: a new Early Ordovician shallow-water fauna with soft-part preservation from China: Science Bulletin, v. 60, p. 812–818.

Bell, M.A., and Lloyd, G.T., 2015, strap: an R package for plotting phylogenies against stratigraphy and assessing their stratigraphic congruence: Palaeontology, v. 58, p. 379–389.

Bergström, J., Stürmer, W., and Winter, G., 1980, *Palaeoisopus, Palaeopantopus* and *Palaeothea*, pycnogonid arthropods from the Lower Devonian Hunsrück Slate, West Germany: Paläontologische Zeitschrift, v. 54, p. 7–54.

Beurlen, K., 1930, Vergleichende Stammesgeschichte. Grundlagen, Methoden, Probleme unter besonderer Berücksichtigung der höheren Krebse: Fortschritte Der Geologie Und Palaeontologie, v. 8, p. 317–586.

Birenheide, R., 1971, Beobachtung am "Scheinsten" *Mimetaster* aus dem Hünsruck–Schiefer: Senckenbergiana Lethae, v. 52, p. 77–91.

Botting, J.P., Muir, L.A., Jordan, N., and Upton, C., 2015, An Ordovician variation on Burgess Shale-type biotas: Scientific Reports, v. 5, p. 1–11.

Brazeau, M.D., Smith, M.R., and Guillerme, T., 2017, MorphyLib: a library for phylogenetic analysis of categorical trait data with inapplicability. https://doi.org/10.5281/zenodo.815372 [October 2021]

Brazeau, M.D., Guillerme, T., and Smith, M.R., 2019, An algorithm for morphological phylogenetic analysis with inapplicable data: Systematic Biology, v. 68, p. 619–631.

Brett, C.E., and Liddell, W.D., 1978, Preservation and paleoecology of a Middle Ordovician hardground community: Paleobiology, v. 4, p. 329–348.

Brett, C.E., Whiteley, T.E., Allison, P.A., and Yochelson, E.L., 1999, The Walcott-Rust Quarry: Middle Ordovician trilobite Konservat-Lagerstätten: Journal of Paleontology, v. 73, p. 288–305.

Briggs, D.E.G., Siveter, D.J., Siveter, D.J., Sutton, M.D., and Legg, D., 2016, Tiny individuals attached to a new Silurian arthropod suggest a unique mode of brood care: Proceedings of the National Academy of Sciences, v. 113, p. 4410–4415.

Briggs, D.E.G., Liu, H.P., Mckay, R.M., and Witzke, B.J., 2018, The Winneshiek biota: exceptionally well-preserved fossils in a Middle Ordovician impact crater: Journal of the Geological Society, v. 175, p. 865–874.

Brookfield, M.E., and Brett, C.E., 1988, Paleoenvironments of the Mid-Ordovician (upper Caradocian) Trenton limestones of southern Ontario, Canada: storm sedimentation on a shoal-basin shelf model: Sedimentary Geology, v. 57, p. 75–105.

Caron, J.-B., and Jackson, D.A., 2008, Paleoecology of the Greater Phyllopod Bed community, Burgess Shale: Palaeogeography, Palaeoclimatology, Palaeoecology, v. 258, p. 222–256.

Caron, J.-B., Rudkin, D.M., and Milliken, S., 2004, A new late Silurian (Pridolian) naraoiid (Euarthropoda: Nektaspida) from the Bertie Formation of southern Ontario, Canada—delayed fallout from the Cambrian explosion: Journal of Paleontology, v. 78, p. 1138–1145.

Cole, S.R., Ausich, W.I., Wright, D.F., and Koniecki, J.M., 2018, An echinoderm Lagerstätte from the Upper Ordovician (Katian), Ontario: taxonomic re-evaluation and description of new dicyclic camerate crinoids: Journal of Paleontology, v. 92, p. 488–505.

Cole, S.R., Wright, D.F., and Ausich, W.I., 2019, Phylogenetic community paleoecology of one of the earliest complex crinoid faunas (Brechin Lagerstätte, Ordovician): Palaeogeography, Palaeoclimatology, Palaeoecology, v. 521, p. 82–98.

Cole, S.R., Wright, D.F., Ausich, W.I., and Koniecki, J.M., 2020, Paleocommunity composition, relative abundance, and new camerate crinoids from the Brechin Lagerstätte (Upper Ordovician): Journal of Paleontology, v. 94, p. 1103–1123.

Conway Morris, S., 1989, The persistence of Burgess Shale-type faunas: implications for the evolution of deeper-water faunas: Earth and Environmental Science Transactions of the Royal Society of Edinburgh, v. 80, p. 271–283.

Farrell, Ú.C., Martin, M.J., Hagadorn, J.W., Whiteley, T., and Briggs, D.E.G., 2009, Beyond Beecher's Trilobite Bed: widespread pyritization of soft tissues in the Late Ordovician Taconic foreland basin: Geology, v. 37, p. 907–910.

Farrell, Ú.C., Briggs, D.E.G., and Gaines, R.R., 2011, Paleoecology of the olenid trilobite *Triarthrus*: new evidence from Beecher's Trilobite Bed and other sites of pyritization: Palaios, v. 26, p. 730–742.

Fritsch, A., 1908, Problematica Silurica, *in* Barrande, J., ed., Système Silurien du Centre de la Bohème: Prague, Bellmann.

Gaines, R.R., 2014, Burgess Shale-type preservation and its distribution in space and time: The Paleontological Society Papers, v. 20, p. 123–146.

Gaines, R.R., Briggs, D.E.G., and Yuanlong, Z., 2008, Cambrian Burgess Shale–type deposits share a common mode of fossilization: Geology, v. 36, p. 755–758.

García-Bellido, D.C., and Collins, D.H., 2006, A new study of *Marrella splendens* (Arthropoda, Marrellomorpha) from the middle Cambrian Burgess Shale, British Columbia, Canada: Canadian Journal of Earth Sciences, v. 43, p. 721–742.

Garm, A., and Watling, L., 2013, The crustacean integument: setae, setules, and other ornamentation, *in* Watling, L., and Thiel, M., eds., Functional Morphology and Diversity: New York, Oxford University Press, p. 167–198.

Goloboff, P.A., and Catalano, S.A., 2016, TNT version 1.5, including a full implementation of phylogenetic morphometrics: Cladistics, v. 32, p. 221–238.

Gupta, N.S., and Briggs, D.E.G., 2011, Taphonomy of animal organic skeletons through time, *in* Allison, P.A., and. Bottjer, D.J., eds., Taphonomy: Dordrecht, Springer, p. 199–221.

Gürich, G., 1931, *Mimetaster hexagonalis*, ein neuer Kruster aus dem unterdevonischen Bundenbacher Dachsiefer: Paläontologische Zeitschrift, v. 13, p. 204–238.

Haug, J.T., Maas, A., and Waloszek, D., 2009, †*Henningsmoenicaris scutula*, †*Sandtorpia vestrogothiensis* gen. et sp. nov. and heterochronic events in early crustacean evolution: Earth and Environmental Science Transactions of the Royal Society of Edinburgh, v. 100, p. 311–350.

Haug, J.T., Castellani, C., Haug, C., Waloszek, D., and Maas, A., 2012, A *Marrella*-like arthropod from the Cambrian of Australia: a new link between "Orsten"-type and Burgess Shale assemblages: Acta Palaeontologica Polonica, v. 58, p. 629–639.

Hearing, T.W., Legg, D.A., Botting, J.P., Muir, L.A., McDermott, P., Faulkner, S., Taylor, A.C., and Brasier, M.D., 2016, Survival of Burgess Shale-type animals in a Middle Ordovician deep-water setting: Journal of the Geological Society, v. 173, p. 628–633.

Hou, X., Clarkson, E.N.K., Yang, J., Zhang, X., Wu, G., and Yuan, Z., 2008, Appendages of early Cambrian *Eoredlichia* (Trilobita) from the Chengjiang biota, Yunnan, China: Earth and Environmental Science Transactions of the Royal Society of Edinburgh, v. 99, p. 213–223.

Kimmig, J., Couto, H., Leibach, W.W., and Lieberman, B.S., 2019, Soft-bodied fossils from the upper Valongo Formation (Middle Ordovician: Dapingian–Darriwilian) of northern Portugal: Science of Nature, v. 106, p. 27.

Kühl, G., and Rust, J., 2010, Re-investigation of *Mimetaster hexagonalis*: a marrellomorph arthropod from the Lower Devonian Hunsrück Slate (Germany): Paläontologische Zeitschrift, v. 84, p. 397–411.

Kühl, G., Bergström, J., and Rust, J., 2008, Morphology, palaeobiology and phylogenetic position of *Vachonisia rogeri* (Arthropoda) from the Lower Devonian Hunsrück Slate (Germany): Palaeontographica Abteilung A, v. 286, p. 123–157.

Lamsdell, J., LoDuca, S.T., Gunderson, G.O., Meyer, R.C., and Briggs, D.E., 2016, A new Lagerstätte from the late Ordovician Big Hill Formation, Upper Peninsula, Michigan: Journal of the Geological Society, v. 174, p. 18–22.

Lankester, E.R., 1904, Memoirs: the structure and classification of the Arthropoda: Quarterly Journal of Microscopical Science, v. 47, p. 523–582.

Legg, D.A., 2015, The morphology and affinities of *Skania fragilis* (Arthropoda) from the middle Cambrian Burgess Shale: Bulletin of Geosciences, v. 90, p. 509–518.

Legg, D.A., 2016a, An acercostracan marrellomorph (Euarthropoda) from the Lower Ordovician of Morocco: Science of Nature, v. 103, p. 21.

Legg, D.A., 2016b, A new marrellid arthropod from the Ordovician of Wales: Acta Palaeontologica Polonica, v. 61, p. 617–619.

Legg, D.A., Sutton, M.D., and Edgecombe, G.D., 2013, Arthropod fossil data increase congruence of morphological and molecular phylogenies: Nature Communications, v. 4, n. 3485, https://doi.org/10.1038/ncomms3485

Lewis, P.O., 2001, A likelihood approach to estimating phylogeny from discrete morphological character data: Systematic Biology, v. 50, p. 913–925.

Liu, Q., 2013, The first discovery of *Marrella* (Arthropoda, Marrellomorpha) from the Balang Formation (Cambrian Series 2) in Hunan, China: Journal of Paleontology, v. 87, p. 391–394.

Macgabhann, B.A., and Murray, J., 2010, Non-mineralised discoidal fossils from the Ordovician Bardahessiagh formation, Co. Tyrone, Ireland: Irish Journal of Earth Sciences, v. 28, p. 1–12.

Maddison, W.P., and Maddison, D.R., 2018, Mesquite: a modular system for evolutionary analysis, version 3.51. http://mesquiteproject.org [October 2021]

Manton, S.M., 1978, Habits, functional morphology and the evolution of pycnogonids: Zoological Journal of the Linnean Society, v. 63, p. 1–21.

Meyer, M.B., Ganis, G.R., Wittmer, J.M., Zalasiewicz, J.A., and De Baets, K., 2018, A Late Ordovician planktic assemblage with exceptionally preserved soft-bodied problematica from the Martinsburg Formation, Pennsylvania: Palaios, v. 33, p. 36–46.

Moysiuk, J., and Caron, J.B., 2019, Burgess Shale fossils shed light on the agnostid problem: Proceedings of the Royal Society B: Biological Sciences, v. 286, n. 20182314, https://doi.org/10.1098/rspb.2018.2314

Muir, L.A., Ng, T.W., Li, X.F., Zhang, Y.D., and Lin, J.P., 2014, Palaeoscolecidan worms and a possible nematode from the Early Ordovician of South China: Palaeoworld, v. 23, p. 15–24.

Muscente, A.D., et al., 2017, Exceptionally preserved fossil assemblages through geologic time and space: Gondwana Research, v. 48, p. 164–188.

Orr, P.J., 2014, Late Proterozoic–early Phanerozoic 'taphonomic windows': the environmental and temporal distribution of recurrent modes of exceptional preservation: The Paleontological Society Papers, v. 20, p. 289–313.

Ortega-Hernández, J., Legg, D.A., and Braddy, S.J., 2013, The phylogeny of aglaspidid arthropods and the internal relationships within Artiopoda: Cladistics, v. 29, p. 15–45.

Paradis, E., Claude, J., and Strimmer, K., 2004, APE: analyses of phylogenetics and evolution in R language: Bioinformatics, v. 20, p. 289–290.

Paton, T.R., and Brett, C.E., 2020, Revised stratigraphy of the middle Simcoe Group (Ordovician, upper Sandbian–Katian) in its type area: an integrated approach: Canadian Journal of Earth Sciences, v. 57, p. 184–198.

Paton, T.R., Brett, C.E., and Kampouris, G.E., 2019, Genesis, modification, and preservation of complex Upper Ordovician hardgrounds: implications for sequence stratigraphy and the Great Ordovician Biodiversification Event: Palaeogeography, Palaeoclimatology, Palaeoecology, v. 526, p. 53–71.

Peel, J.S., Willman, S., and Pedersen, S.A.S., 2019, Unusual preservation of an Ordovician (Floian) arthropod from Peary Land, North Greenland (Laurentia): Paläontologische Zeitschrift, v. 94, p. 41–51.

R Core Team, 2020, R: a language and environment for statistical computing. https://www.R-project.org/ [October 2021]

Rak, Š., Ortega-Hernández, J., and Legg, D.A., 2013, A revision of the Late Ordovician marrellomorph arthropod *Furca bohemica* from Czech Republic: Acta Palaeontologica Polonica, v. 58, p. 615–628.

Rambaut, A., Surchard, M.A., Xie, D., and Drummond, A.J., 2014, Tracer v1.6. http://Beast.Bio.Ed.Ac.Uk/Tracer [October 2021]

Raymond, P.E., 1920, The appendages, anatomy, and relationships of trilobites: Memoirs of the Connecticut Academy of Arts and Sciences, v. 7, 169 p.

Ronquist, F., Van Der Mark, P., Teslenko, M., Ayres, D.L., Darling, A., Höhna, S., Larget, B., Liu, L., Suchard, M.A., and Huelsenbeck, J.P., 2012, MrBayes 3.2: Efficient bayesian phylogenetic inference and model choice across a large model space: Systematic Biology, v. 61, p. 539–542.

Rust, J., Bergmann, A., Bartels, C., Schoenemann, B., Sedlmeier, S., and Kühl, G., 2016, The Hunsrück biota: a unique window into the ecology of Lower Devonian arthropods: Arthropod Structure & Development, v. 45, p. 140–151.

Schliep, K.P., 2011, phangorn: phylogenetic analysis in R: Bioinformatics, v. 27, p. 592–593.

Schram, F.R., and Hedgpeth, J.W., 1978, Locomotory mechanisms in Antarctic pycnogonids: Zoological Journal of the Linnean Society, v. 63, p. 145–169.

Seilacher, A., Reif, W.E., and Westphal, F., 1985, Sedimentological, ecological and temporal patterns of fossil Lagerstätten: Philosophical Transactions of the Royal Society of London B: Biological Sciences, v. 311, p. 5–24.

Sharma, P.P., Clouse, R.M., and Wheeler, W.C., 2017, Hennig's semaphoront concept and the use of ontogenetic stages in phylogenetic reconstruction: Cladistics, v. 33, p. 93–108.

Siveter, D.J., Sutton, M.D., Briggs, D.E.G., and Siveter, D.J., 2004, A Silurian sea spider: Nature, v. 431, p. 978–980.

Siveter, D.J., Fortey, R.A., Sutton, M.D., Briggs, D.E.G., and Siveter, D.J., 2007, A Silurian marrellomorph arthropod: Proceedings of the Royal Society B: Biological Sciences, v. 274, p. 2223–2229.

Siveter, D.J., Briggs, D.E.G., Siveter, D.J., and Sutton, M.D., 2020, The Herefordshire Lagerstätte: fleshing out Silurian marine life: Journal of the Geological Society, v. 177, p. 1–13.

Smith, M.R., 2018, TreeSearch: phylogenetic tree search using custom optimality criteria. https://doi.org/10.5281/zenodo.1042590 [October 2021]

Smith, M.R., 2019a, TreeTools: create, modify and analyse phylogenetic trees. https://doi.org/10.5281/zenodo.3522725 [October 2021]

Smith, M.R., 2019b, Bayesian and parsimony approaches reconstruct informative trees from simulated morphological datasets: Biology Letters, v. 15, n. 20180632, https://doi.org/10.1098/rsbl.2018.0632

Størmer, L., 1959, Trilobitoidea, *in* Moore, R.C., ed., Treatise on Invertebrate Paleontology, Part O, Arthropoda 1: Boulder, Colorado, and Lawrence, Kansas, Geological Society of America and University of Kansas Press, p. O23–O37.

Stott, C.A., Tetlie, O.E., Braddy, S.J., Nowlan, G.S., Glasser, P.M., and Devereux, M.G., 2005, A new eurypterid (Chelicerata) from the Upper Ordovician of Manitoulin Island, Ontario, Canada: Journal of Paleontology, v. 79, p. 1166–1174.

Vannier, J., Aria, C., Taylor, R.S., and Caron, J.-B., 2018, *Waptia fieldensis* Walcott, a mandibulate arthropod from the middle Cambrian Burgess Shale: Royal Society Open Science, v. 5, n. 172206, https://doi.org/10.1098/rsos.172206

Van Roy, P., 2006, Non-trilobite arthropods from the Ordovician of Morocco [Ph.D. thesis]: Ghent, Ghent University, 230 p.

Van Roy, P., Orr, P.J., Botting, J.P., Muir, L.A., Vinther, J., Lefebvre, B., el Hariri, K., and Briggs, D.E.G., 2010, Ordovician faunas of Burgess Shale type: Nature, v. 465, p. 215–218.

Van Roy, P., Briggs, D.E.G., and Gaines, R.R., 2015, The Fezouata fossils of Morocco; an extraordinary record of marine life in the Early Ordovician: Journal of the Geological Society, v. 172, p. 541–549.

von Bitter, P.H., Purnell, M.A., Tetreault, D.K., and Stott, C.A., 2007, Eramosa Lagerstätte—exceptionally preserved soft-bodied biotas with shallow-marine shelly and bioturbating organisms (Silurian, Ontario, Canada): Geology, v. 35, p. 879–882.

Walcott, C.D., 1912, Cambrian geology and paleontology 2, no. 6. Middle Cambrian Branchiopoda, Malacostraca, Trilobita, and Merostomata: Smithsonian Miscellaneous Collections, v. 57, p. 145–229.

Whittington, H.B., 1971, Redescription of *Marrella splendens* (Trilobitoidea) from the Burgess Shale, middle Cambrian, British Columbia: Bulletin of Geological Survey of Canada, v. 209, p. 1–24.

Wolodzko, T., 2020, extraDistr: additional univariate and multivariate distributions. R package version 1.9.1. https://github.com/twolodzko/extraDistr [October 2021]

Wright, D.F., Cole, S.R., and Ausich, W.I., 2020, Biodiversity, systematics, and new taxa of cladid crinoids from the Ordovician Brechin Lagerstätte: Journal of Paleontology, v. 94, p. 334–357.

Young, G.A., Rudkin, D.M., Dobrzanski, E.P., Robson, S.P., Cuggy, M.B., Demski, M.W., and Thompson, D.P., 2012, Great Canadian Lagerstätten 3. Late Ordovician Konservat-Lagerstätten in Manitoba: Geoscience Canada, v. 39, p. 201–213.

Zeng, H., Zhao, F., Niu, K., Zhu, M., and Huang, D., 2020, An early Cambrian euarthropod with radiodont-like raptorial appendages: Nature, v. 588, p. 101–105.